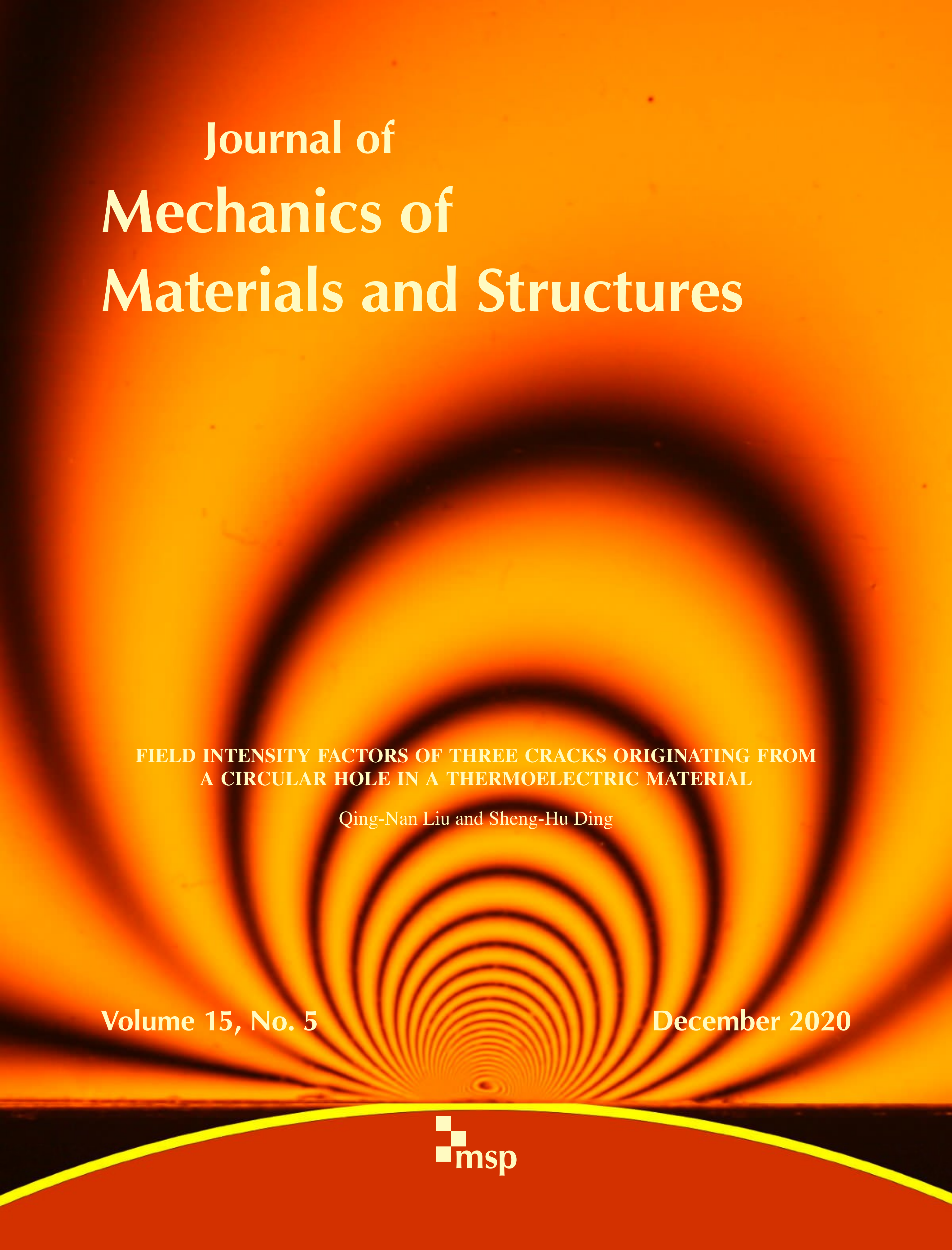

Journal of
Mechanics of Materials and Structures

FIELD INTENSITY FACTORS OF THREE CRACKS ORIGINATING FROM A CIRCULAR HOLE IN A THERMOELECTRIC MATERIAL

Qing-Nan Liu and Sheng-Hu Ding

Volume 15, No. 5 December 2020

msp

JOURNAL OF MECHANICS OF MATERIALS AND STRUCTURES
Vol. 15, No. 5, 2020
https://doi.org/10.2140/jomms.2020.15.605

FIELD INTENSITY FACTORS OF THREE CRACKS ORIGINATING FROM A CIRCULAR HOLE IN A THERMOELECTRIC MATERIAL

QING-NAN LIU AND SHENG-HU DING

The fracture behavior of three cracks originating from a circular hole in a thermoelectric material is studied. The basic theory of thermoelectric materials is given under the condition of the impermeable boundary of the heat flux and electric current. By introducing the conformal mapping function, the infinite plane on the physical plane is mapped into the inner unit circle on the mathematical plane. The formulas of the relevant temperature and stress fields are derived, and the analytical solutions of the complex stress functions are obtained by the complex variable function method. According to Cauchy integral formula, the analytical expressions of the electric current intensity factor and the stress intensity factor for three cracks originating from a circular hole are obtained. The effects of the hole radius and the crack lengths on the electric current intensity factor and stress intensity factors were investigated.

1. Introduction

Thermoelectric materials are functional materials that directly convert thermal energy to electric energy through the movement of a solid internal carrier. They are widely used in energy, refrigeration, microelectronics, aerospace military and other fields [Hone et al. 2013; Wu et al. 2018; Roncaglia and Ferri 2011; Wang et al. 2014; Liu et al. 2017]. Thermoelectric materials also have important applications in thermoelectric power generation [Roncaglia and Ferri 2011], such as industrial waste heat recovery and waste heat recovery systems, solid-state thermal management, solar energy collection, carbon emission reduction [Pierce and Vaudo 2010], automobile exhaust, etc.

Thermoelectric materials have become an important branch of modern functional materials [Narasimha et al. 2014; Yu et al. 2018]. However, thermoelectric materials are brittle materials. Due to the mechanical, thermal and electrical factors, cracks or microcracks will inevitably occur in the machining process [Bigoni and Movchan 2002; Xie et al. 2017; Shi 2020]. Craciun et al. [2014] studied the mode II fracture problem of an anisotropic unbounded elastic body with three collinear equal cracks. The effect of thermal load on the stress intensity factors of a finite length edge crack in an orthotropic infinite strip with finite thickness is studied by Singh et al. [2019] Therefore, the research on fracture or cracks in thermoelectric materials has important theoretical and practical significance. In recent years, some scholars have studied the theory and methods of cracks in thermoelectric materials. Using the complex function method, the two-dimensional problem of cracks in thermoelectric materials was studied in [Song et al. 2015], and the effect of a crack on the conversion efficiency of thermoelectric materials was discussed in [Song and Song 2016]. Considering the electrically and thermally impermeable crack model, Zhang and Wang

Sheng-Hu Ding is the corresponding author.
Keywords: thermoelectric material, circular hole, three cracks, complex variable function, intensity factors.

[2013] studied the crack problem in a medium possessing a coupled thermoelectric effect under thermal-electric loads. Considering the electric impermeable and heat semi-permeable crack model, the interface crack problem in a layered thermoelectric material is investigated in [Zhang and Wang 2016b]. By using the integral equation method, the thermal conductivity models of multilayer thermoelectric plates with Griffith cracks and non-collinear cracks under different loads are established in [Ding and Liu 2018; Ding and Zhou 2018]. The influence of the strip width of thermoelectric materials on the electric flux intensity factor and the heat flux intensity factor was studied. The general model of a bi-layered thermoelectric composite system with an interfacial crack is considered and the effect of interfacial cracking on the thermoelectric properties is investigated in [Wang et al. 2018]. Clin et al. [2009] studied the stress distribution of a thermocouple via numerical simulation. Turenne et al. [2010] studied the effects of the boundary conditions and the length of the thermocouple on the stress distribution of thermoelectric devices by numerical simulation. A finite element computational scheme for transient and nonlinear coupling thermoelectric fields and the associated thermal stresses in thermoelectric materials is studied in [Wang 2017].

As we all know, the holed structures play an important role in engineering. In the process of manufacturing and using a holed structure, cracks often appear around the hole [Tada et al. 1973; Ouchterlony 1976; Wu and Carlsson 1991]. In addition, when thermoelectric materials are subjected to thermal and electrical loads, the stress concentration near the hole will initiate and propagate cracks, which will lead to the failure of thermoelectric materials. Therefore, it is necessary and important to analyze the fracture behavior of thermoelectric materials, especially those with holes and cracks. For isotropic materials, the problem of multiple radial cracks originating from a circular hole using the complex variable method is studied in [Bowie 1956]. The problem of one and two cracks at the edge of an elliptic hole in an infinite isotropic material is solved using the integral transforms method from [Tweed and Melrose 1989]. Bertoldi et al. [2007] solved the problem of elliptical inclusions connected by the structural interface to an infinite matrix analytically. For the case of anisotropic materials, the solutions of the stress intensity factors of a single or two collinear edge cracks emanating from a curvilinear hole in an infinite anisotropic plane based on the boundary element method is investigated in [Liaw and Kamel 1991]. Zhang and Wang [2016a] solved the two-dimensional problem of an elliptical hole in thermoelectric materials by using the complex function method. The results show that the thermoelectric conversion efficiency can be higher than the maximum conversion efficiency of one-dimensional thermocouples at the same temperature when the current flow and heat flux are separated. The theoretical model of thermoelectric coupling for thermoelectric materials with inclined elliptical holes is established in [Wang and Wang 2017]. The effective properties of a thermoelectric material in the vicinity of an arbitrarily shaped hole are studied in [Song et al. 2019b]. The contribution of surface elasticity and electric current density on the thermal stress distribution around a circular nano-hole in a thermoelectric material is considered in [Song et al. 2019a]. Using complex variable methods, the closed-form solutions describing the corresponding thermoelastic fields in the vicinity of the nano-hole are given. Using the complex variable function method and the conformal mapping technique, the model of infinite thermoelectric material containing a circular hole with a straight crack is considered in [Pang et al. 2018]. Using the same method, Jiang et al. [2020] studied the two-dimensional problem of a circular hole with two unequal cracks in an infinite thermoelectric material under the action of uniform current and heat flux. However, the above two papers are both thermoelectric uncoupled model, which is inconsistent with the actual engineering situation. In fact, thermoelectric material is coupled by thermal field and electric field. Therefore, considering the thermoelectric coupling effect, this paper studied the problem of three cracks at the edge of a circular hole in thermoelectric material. The effects of various parameters on current intensity factor and stress intensity factor are given.

The purpose of the present work to study the fracture problem of three cracks originating from a circular hole in a thermoelectric material under combined thermal and electrical loads. In addition, it is very interesting and challenging to obtain the analytical solutions for such complicated crack problems, since these solutions can provide the theoretical bases for fracture problems in thermoelectric materials, and can also be used as benchmark approximate methods to judge the accuracy and effciency of various numerical methods.

2. Basic equations

2.1. ***Governing equations.*** Consider an infinite thermoelectric material in which all fields are assumed to depend only on the in-plane coordinates x and y. When no free electric charge and heat source exist, the coupled transports equations of the heat and electrons in a thermoelectric material were given by [Perez-Aparicio et al. 2007]

$$\boldsymbol{J}_q = -\left(\frac{T^2\gamma\varepsilon}{e}\right)\frac{1}{T}\nabla V + (T^3\gamma\varepsilon^2 + T^2k)\nabla\frac{1}{T}, \tag{1}$$

$$\boldsymbol{J}_u = \left(\frac{T^2\gamma\varepsilon}{e}\right)\nabla\frac{1}{T} - \left(\frac{T\gamma}{e^2}\right)\frac{1}{T}\nabla V, \tag{2}$$

where $V = e\nu$, and the electric current density $\boldsymbol{J}_e$ is coupled with the heat flux $\boldsymbol{J}_q$ through the Seebeck coefficient ε. $\boldsymbol{J}_u$ is the energy flux. In the thermoelectric materials, the electric current density can be derived from the energy flux, where $\boldsymbol{J}_e = e\boldsymbol{J}_u$. In addition T, ν, γ, k are the temperature, electric potential, electrical conductivity and thermal conductivity.

It is easy to find that

$$\boldsymbol{J}_e = -\gamma\nabla\nu - \gamma\varepsilon\nabla T, \tag{3}$$

$$\boldsymbol{J}_q = -\gamma\varepsilon T\nabla\nu - (\gamma\varepsilon^2 T + k)\nabla T. \tag{4}$$

The energy flux can be expressed as

$$\boldsymbol{J}_u = \boldsymbol{J}_q + \boldsymbol{J}_e\nu. \tag{5}$$

Assuming that the energy and charge in thermoelectric materials are all conserved, the electric current density and energy flux have the form

$$\nabla\cdot\boldsymbol{J}_e = 0, \tag{6}$$

$$\nabla\cdot\boldsymbol{J}_q + \boldsymbol{J}_e\cdot\nabla\nu = 0. \tag{7}$$

2.2. ***General solution of the thermoelectric field.*** A new function F is introduced as

$$F = \nu + \varepsilon T. \tag{8}$$

Then the constitutive equations can be rewritten as

$$\boldsymbol{J}_e = -\gamma \nabla F, \tag{9}$$

$$\boldsymbol{J}_u = -\gamma F \nabla F - k \nabla T. \tag{10}$$

For the solution of two-dimensional problems in thermoelectric materials, the temperature field and electric field can be expressed by two decomposed complex functions. Substituting (9) and (10) into (6) and (7) respectively, the governing equations become

$$\nabla^2 F = 0, \tag{11}$$

$$k \nabla^2 T + \gamma (\nabla F)^2 = 0. \tag{12}$$

Following [Muskhelishvili 1975], let F be the real part of the analytic complex function $f_1(z)$, where $z = x + iy$. We get

$$F = \mathrm{Re}[f_1(z)]. \tag{13}$$

Substituting (13) into (9), we obtain

$$\begin{aligned} J_{ex} &= -\gamma \mathrm{Re}[f_1(z)]_x = -\frac{1}{2}\gamma\big(f_1'(z) + \overline{f_1'(z)}\big), \\ J_{ey} &= -\gamma \mathrm{Re}[f_1(z)]_y = -\frac{i}{2}\gamma\big(f_1'(z) - \overline{f_1'(z)}\big). \end{aligned} \tag{14}$$

or

$$J_{ex} - i J_{ey} = -\gamma f_1'(z). \tag{15}$$

From (3) and (6), we get

$$\boldsymbol{J}_e{}^2 = -\gamma k \nabla^2 T = \frac{\gamma k \nabla^2 \nu}{\varepsilon}. \tag{16}$$

Namely

$$\nabla^2 T = -\frac{\gamma}{k}[\nabla \mathrm{Re}[f_1(z)]]^2 = -\frac{\gamma}{k} f_1'(z)\overline{f_1'(z)}. \tag{17}$$

Considering the two-dimensional thermoelectric problem, the temperature field is superposed by two functions

$$T = T_1 + T_2, \tag{18}$$

where T_1 and T_2 satisfy

$$\nabla^2 T_1 = -\frac{\gamma}{k} f_1'(z)\overline{f_1'(z)}\,, \tag{19}$$

$$\nabla^2 T_2 = 0. \tag{20}$$

By integrating (17), we have

$$T = -\frac{\gamma}{4k} f_1(z)\overline{f_1(z)} + \mathrm{Re}[g(z)], \tag{21}$$

where $g(z)$ is an arbitrary analytic function.

From (10) and (18), the energy flux can be expressed as

$$J_{ux} - i J_{uy} = -\frac{\gamma}{2} f_1(z) f_1'(z) - k g'(z). \tag{22}$$

2.3. *General solution of the stress field.* For plane problems, combined with the compatibility equation, the stress function Φ satisfies

$$\nabla^4 \Phi = -\beta \nabla^2 T, \tag{23}$$

where β is a coefficient taking the value $E\alpha$ for plane stress and $E\alpha/(1-\nu)$ for plane strain, where E, ν, α are the Young's modulus, Poisson ratio and thermal expansion coefficient.

For planar two-dimensional problems, the stress function Φ is written as two complex decomposition functions,

$$\Phi(x, y) = \psi(x, y) + \psi_0(x, y), \tag{24}$$

where $\psi(x, y)$ is the special solution of the stress function, and $\psi_0(x, y)$ is the general solution of the stress function. Combining (20) and (21) with (23), we obtain

$$\psi = -\frac{\gamma \beta f_2(z) \overline{f_2(z)}}{16k}, \tag{25}$$

where $f_2'(z) = f_1(z)$.

According to the superposition principle, the stresses and displacements can be expressed as

$$\begin{aligned} \sigma_{xx} + \sigma_{yy} &= 4\mathrm{Re}[\varphi'(z)] + \frac{\mu\beta\gamma}{2k} f_1(z)\overline{f_1(z)}, \\ \sigma_{yy} - \sigma_{xx} + 2i\sigma_{xy} &= 2[\bar{z}\varphi''(z) + \phi'(z)] + \frac{\mu\beta\gamma}{2k} f_2(z)\overline{f_1'(z)}, \end{aligned} \tag{26}$$

$$2\mu[u_x + iu_y] = \kappa\varphi(z) - z\overline{\varphi'(z)} - \overline{\phi(z)} + 2\mu\alpha^* \int g(z)\,dz - \frac{\mu\beta\gamma}{4k} f_2(z)\overline{f_1(z)}, \tag{27}$$

where $\varphi(z)$ and $\phi(z)$ are complex stress functions, κ and α^* are defined as follows

$$\begin{aligned} \alpha^* &= \begin{cases} \alpha, & \text{for plane stress state} \\ (1+v)\alpha. & \text{for plane strain state} \end{cases} \\ \kappa &= \begin{cases} 3-v\big/1+v, & \text{for plane stress state} \\ 3-4v. & \text{for plane strain state} \end{cases} \end{aligned} \tag{28}$$

The boundary condition of the stress in thermoelectric materials can be expressed as

$$\varphi(z) + z\overline{\varphi'(z)} + \overline{\phi(z)} = i \int (p_x + ip_y)\,ds - \frac{\mu\beta\gamma}{4k} f_2(z)\overline{f_1(z)} + \text{constant}, \tag{29}$$

where the constants p_x and p_y are the external forces exerted on the boundary, and they are assumed to be zero.

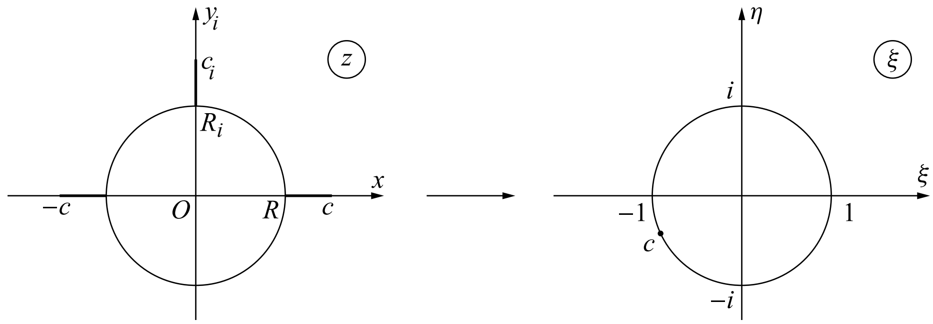

Figure 1. A circular hole with three cracks in thermoelectric material for z-plane and ξ-plane.

3. Thermoelectric field for a circular hole with three cracks

3.1. ***Formulation of problems.*** Consider a circular hole with three equal-length cracks on an infinite plane. The radius of the circle is R and the length of the crack is $c-R$. The boundary conditions on the circular hole surfaces are regarded as electrically and thermally insulated. The medium is subjected to a uniform electric current density and a uniform heat flux at infinity. Thus, the boundary conditions can be expressed as

$$\begin{cases} J_{qx}=0,\ J_{qy}=0, & |z|=R \text{ or } R<|x|<c \text{ or } R<|y|<c, \\ J_{ex}=0,\ J_{ey}=0, & |z|=R \text{ or } R<|x|<c \text{ or } R<|y|<c, \\ J_{ex}=0,\ J_{ey}=J_{e0}, & |x|\to\infty,\ |y|\to\infty, \\ J_{ux}=0,\ J_{uy}=J_{u0}. & |x|\to\infty,\ |y|\to\infty. \end{cases} \tag{30}$$

As shown in Figure 1, we transform the exterior of a circular hole with three cracks in the z-plane into the interior of a unit circle on the ξ-plane by introducing the conformal mapping function $z=\omega(\xi)$ by

$$z=\omega(\xi)=\frac{R}{2\xi}\Big[\sqrt{-m_1\xi^2+m_2(\xi^2+1)^2}+\sqrt{-m_1\xi^2-4\xi^2+m_2(\xi^2+1)^2}\,\Big], \tag{31}$$

where

$$m_1=\frac{(c^2-R^2)^2}{R^2c^2},\qquad m_2=\frac{c^4+R^4}{2R^2c^2}, \tag{32}$$

in which $\sqrt{-1}=\mathrm{i}$, and we take $\omega^{-1}(c)\to 1,\ \omega^{-1}(-c)\to -1,\ \omega^{-1}(ci)\to c.$

Substituting (31) into (26) and (29), we have

$$\begin{aligned} \sigma_\theta+\sigma_\rho&=4\mathrm{Re}\Big[\frac{\varphi'(\zeta)}{\omega'(\zeta)}\Big]+\frac{\mu\beta\gamma}{2k}f_1(z)\overline{f_1(z)}, \\ \sigma_{yy}-\sigma_{xx}+2i\sigma_{xy}&=2\Big[\bar z\Big(\frac{\varphi'(\zeta)}{\omega'(\zeta)}\Big)'+\frac{\phi'(\zeta)}{\omega'(\zeta)}\Big]+\frac{\mu\beta\gamma}{2k}f_2(z)\overline{f_1'(z)}, \end{aligned} \tag{33}$$

$$\phi(\zeta)+\frac{w(\zeta)}{\overline{w'(\zeta)}}\overline{\phi'(\zeta)}+\overline{\varphi(\zeta)}=i\int(p_x+ip_y)\,ds-\frac{\mu\beta\gamma}{4k}f_2(\zeta)\overline{f_1(\zeta)}+\text{constant}, \tag{34}$$

where θ and ρ are the polar angle and polar radius of the polar coordinates at the crack tip of the ξ-plane.

3.2. ***Solution of the cracks.*** To solve the two-dimensional plane crack problem, the boundary conditions of the circular surfaces are electrically and thermally insulated, and the material plate is subjected to a uniform electric current density ($J_{ex}=0,\ J_{ey}=J_{e0}$) and an energy flux ($J_{ux}=0,\ J_{uy}=J_{u0}$) at infinity. When the potential difference and temperature difference are given, the current density and energy flux in the thermoelectric material are constantly distributed, and the heat flux is non-linear with spatial coordinates. Therefore, it is more convenient to use J_{e0} and J_{u0} to solve the far-field thermoelectric boundary conditions for circular hole problems with the boundary conditions of the electric current density and energy flux given by

$$f_1(z)-\overline{f_1(z)}=-\int J_{en}(s)\,ds+\text{constant}, \tag{35}$$

$$\mathrm{Im}\Big[\frac{\gamma}{4}f_1^2(z)+\kappa g(z)\Big]=-\int J_{un}(s)\,ds+\text{constant}, \tag{36}$$

where n indicates the normal direction, J_{en} and J_{un} stand for the electric current density and energy flux in the direction normal to s, respectively.

With considering the electric current impermeable cracks and the boundary conditions of the current density insulation at the edge of the hole, (35) can be rewritten as

$$f_1(z)-\overline{f_1(z)}=0. \tag{37}$$

According to the electric current density condition at infinity, the complex function $f_1(z)$ can be expressed as

$$f_1(z)=a_1z+f_0(z), \tag{38}$$

where a_1 is a complex constant related to the electric current density at infinity and $f_0'(\infty)=0$.

Substituting (38) into (15), and then taking the limit $z\to\infty$ gives

$$a_1=\frac{iJ_{e0}}{\gamma}. \tag{39}$$

Substituting (31) and (39) into (37) and noting $\xi=\sigma=e^{i\theta}$ on the circular surface, we have

$$f_0(\sigma)-\overline{f_0(\sigma)}=-\frac{iJ_{e0}\mathrm{R}}{2\sigma\gamma}\big[\sqrt{-4m_1\sigma^2+4m_2(\sigma^2+1)^2}+\sqrt{-4m_1\sigma^2-16\sigma^2+4m_2(\sigma^2+1)^2}\big]. \tag{40}$$

Multiplying both sides of (40) by $\frac{1}{2\pi\mathrm{i}}\frac{d\sigma}{\sigma-\xi}$ and carrying out the Cauchy integration yields, we obtain

$$f_0(\zeta)=-i\frac{2J_{e0}}{\gamma}\Big[w(\zeta)-\frac{R\sqrt{m_2}}{\xi}\Big]. \tag{41}$$

Substituting (31) and (41) into (38), we have

$$f_1(z)=-\frac{iJ_{e0}R}{2\gamma\xi}\big[\sqrt{-m_1\xi^2+m_2(\xi^2+1)^2}+\sqrt{-m_1\xi^2-4\xi^2+m_2(\xi^2+1)^2}-4\sqrt{m_2}\big]. \tag{42}$$

From (21) and (42), the function $g(z)$ related to the temperature function can be expressed as

$$g(z)=a_2z^2+b_2z+g_0(z), \tag{43}$$

where a_2 and b_2 respectively represent the complex constants of the electric current density and energy flux at infinity, and $g_0'(\infty)=0$

Substituting (42) and (43) into (22), and then taking the limit $z\to\infty$ gives

$$a_2=\frac{{J_{e0}}^2}{4k\gamma},\ b_2=\frac{iJ_{u0}}{k}. \tag{44}$$

Substituting (42) and (44) into (36), considerating $\xi=\sigma=e^{i\theta}$ on the circular surface and $J_{un}=0$, and carrying out the Cauchy integration yields

$$g(z)=-\frac{iJ_{u0}R}{2k\xi}\big[\sqrt{-m_1\xi^2+m_2(\xi^2+1)^2}+\sqrt{-m_1\xi^2-4\xi^2+m_2(\xi^2+1)^2}-4\sqrt{m_2}\big]$$

$$\frac{{J_{e0}}^2R^2}{16k\gamma}\big[-2m_1+2m_2(\zeta+\zeta^{-1})^2-4+\sqrt{[-m_1+m_2(\zeta+\zeta^{-1})^2]^2+16m_1-16m_2(\zeta+\zeta^{-1})^2}\big]. \tag{45}$$

Considering the problem of two-dimensional thermal stresses, the complex potentials $\varphi(\zeta)$ and $\phi(\zeta)$ in thermoelectric material have the form

$$\varphi(\zeta)=A_1(\zeta)\ln\zeta+\varphi_0(\zeta),\quad \phi(\zeta)=A_2(\zeta)\ln\zeta+\phi_0(\zeta), \tag{46}$$

where $A_1(\xi)$ and $A_2(\xi)$ are unknown complex functions at infinity.

Substituting (46) into (34), we obtain

$$\begin{aligned}A_1(\xi)&=R^2m_2A_0,\\ A_2(\xi)&=\overline{A}_1+2R^3P_0\big[\sqrt{4m_2(\xi+\xi^{-1})^2-4m_1}+\sqrt{4m_2(\xi+\xi^{-1})^2-4m_1-16}\big],\end{aligned} \tag{47}$$

where

$$A_0=-\frac{2\mu\alpha^*iJ_{u0}}{k(\kappa+1)},\qquad P_0=\frac{\mu\beta J_{e0}^2}{8k\gamma}. \tag{48}$$

By setting p_x and p_y as zero, the stress boundary condition in (34) can be rewritten as

$$\varphi(\sigma)+\frac{\omega(\sigma)}{\overline{\omega'(\sigma)}}\overline{\varphi'(\sigma)}+\overline{\phi(\sigma)}=-\frac{\mu\beta\gamma}{4k}f_2(\sigma)\overline{f_1(\sigma)}. \tag{49}$$

From (31), we have

$$\omega'(\zeta)=m_2R(\zeta+\zeta^{-1})(1-\zeta^{-2})[(-4m_1+4m_2(\zeta+\zeta^{-1})^2)^{-\frac{1}{2}}+(-4m_1+4m_2(\zeta+\zeta^{-1})^2-16)^{-\frac{1}{2}}], \tag{50}$$

which leads to the following expression for $M=\omega(\xi)/\overline{\omega'(\xi)}$:

$$M=\frac{R}{4\xi}\frac{\sqrt{4m_2(\xi^2+1)^2-4m_1\xi^2}+\sqrt{4m_2(\xi^2+1)^2-4m_1\xi^2-16\xi^2}}{m_2R(\xi+\xi^{-1})(1-\xi^2)\big[(4m_2(\xi+\xi^{-1})^2-4m_1)^{-\frac{1}{2}}+(4m_2(\xi+\xi^{-1})^2-4m_1-16)^{-\frac{1}{2}}\big]} \tag{51}$$

It can be deduced that $\omega'(\xi)$ and $\frac{w(\zeta)}{w'(\zeta)}\overline{\varphi_0'(\zeta)}$ are analytically outside the unit circle and can be extended to an analytic function on the circle. Then using of the Cauchy integral at infinity leads to

$$\frac{1}{2\pi i}\int_\sigma\frac{w(\sigma)}{w'(\sigma)}\frac{\overline{\varphi_0'(\sigma)}}{\sigma-\zeta}d\sigma=0. \tag{52}$$

Note that on the circular surface, we have $\xi=\sigma=\mathrm{e}^{i\theta}$. Then, substituting (51) and (52) into (49) and carrying out the Cauchy integration yields

$$\varphi_0(\xi)=\frac{R^2m_2\overline{A}_0}{\zeta},\quad \phi_0(\xi)=(8R^3p_0\sqrt{m_2}+R^2m_2\overline{A}_0)\zeta^{-1}. \tag{53}$$

From (46) and (53), $\varphi(\zeta)$ and $\phi(\zeta)$ can be expressed as

$$\varphi(\xi)=m_2R^3p_0\zeta\big[4\sqrt{m_2}\zeta^{-1}-8\sqrt{m_2}(\zeta^2+\zeta^{-2}) \\ +\sqrt{-4m_1\zeta^2+4m_2(\zeta^2{+}1)^2}+\sqrt{-4m_1\zeta^2-16\zeta^2+4m_2(\zeta^2{+}1)^2}\big], \tag{54}$$

$$\phi(\zeta)=m_2R^3p_0\zeta\big[\sqrt{-4m_1\zeta^2+4m_2(\zeta^2{+}1)^2} \\ +4\sqrt{m_2}(\zeta^{-1}-2\zeta^{-4}-2)+\sqrt{-4m_1\zeta^2-16\zeta^2+4m_2(\zeta^2+1)^2}\big]-\overline{M_2}\varphi_0'(\zeta). \tag{55}$$

For the problem of hole edge cracks, the current intensity factors at the crack tip c are defined as

$$\begin{aligned}K_e=K_{ex}-iK_{ey}&=\lim_{z\to R+c}\sqrt{2\pi(z-R-c)}(J_{ex}-iJ_{ey})\\ &=-\gamma\lim_{\xi\to 1}\sqrt{2\pi[\omega(\xi)-\omega(1)]}\frac{f_1'(\xi)}{\omega'(\xi)}.\end{aligned} \tag{56}$$

Substituting (42) and (54) into (56), we have

$$K_e=K_{ex}-iK_{ey}=i\sqrt{\pi R}\sqrt{\frac{c^4+R^4}{Rc}}j_{e0}. \tag{57}$$

For the problem of hole edge cracks, the stress intensity factor at the crack tip c can be expressed as

$$K_I-iK_{II}=\lim_{z\to R+c}2\sqrt{2\pi(\omega(\xi)-R-c)}\varphi'(z)=\lim_{\xi\to 1}2\sqrt{2\pi(\omega(\xi)-\omega(1))}\frac{\varphi'(\xi)}{\omega'(\xi)}. \tag{58}$$

Substituting (50) and (54) into (58), we have

$$K_I=\frac{m_2R^3\mu\beta J_{e0}^2}{8k\gamma}\sqrt{\frac{\pi}{c}}\bigg(\frac{16m_2-2m_1}{\sqrt{16m_2-4m_1}}+\frac{16m_2-2m_1-8}{\sqrt{16m_2-4m_1-16}}-8\sqrt{m_2}\bigg)., \tag{59}$$

$$K_{II}=\frac{\mu\alpha^*J_{u0}}{k(\kappa+1)}\sqrt{\frac{\pi}{c}}\frac{c^4+R^4}{c^2}. \tag{60}$$

Under limiting conditions, the new configuration can be simulated from the present result. If the length of crack c-R tends to zero, using (42), (15) reduces to

$$J_{ex}-\mathrm{i}J_{ey}=\mathrm{i}J_{e0}\frac{1+\bar{\xi}^2}{\bar{\xi}\xi^{-2}} \tag{60}$$

which is the result for an infinite thermoelectric material containing only a circular hole [Zhang and Wang 2016a].

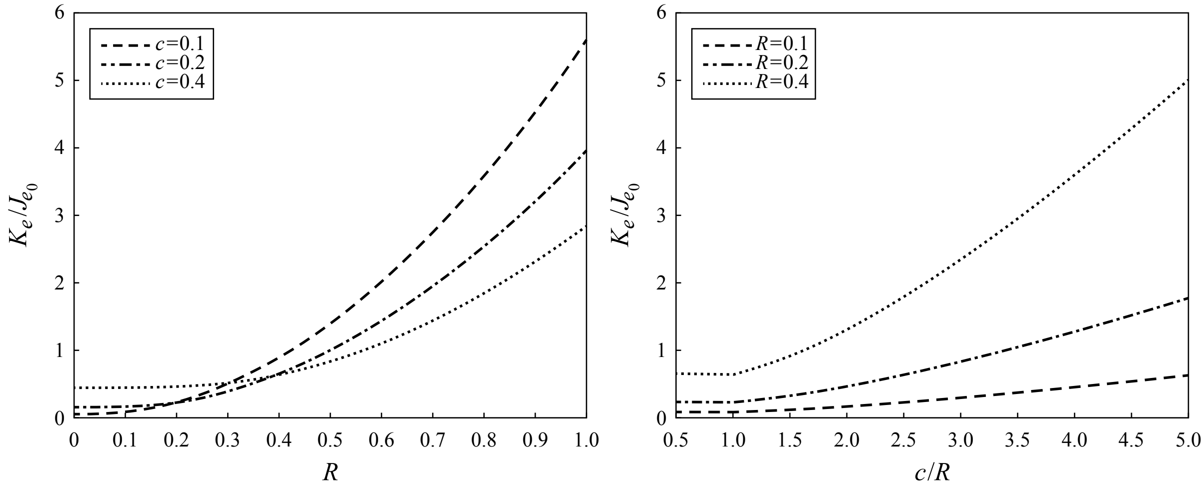

Figure 2. Variation of the electric intensity factor K_e with R (left) and c/R (right).

4. Numerical examples

When an infinite thermoelectric plate with three cracks originating from circular hole is subjected to a uniform current at infinity, the electric intensity factor at the crack tip c is shown in Figure 2. From (57), it can be seen that the electric intensity factor is related not only to the radius R of the circle, but also to the length c/R of the crack. When the radius of the circular hole is larger and other conditions remain unchanged, the electric intensity factor K_e at the crack tip increases as R increases, and the change speed becomes faster as R increases. When R is a constant value, the electric intensity factor K_e at the crack tip increases with an increase of c/R, and the change speed becomes faster as R increases. Figure 3 shows the variation of the stress intensity factor K_I at the crack tip c with parameters R/c and R. It can be found that when the orifice radius is constant, c/R increases as the value of K_I increases. When R/c is a fixed

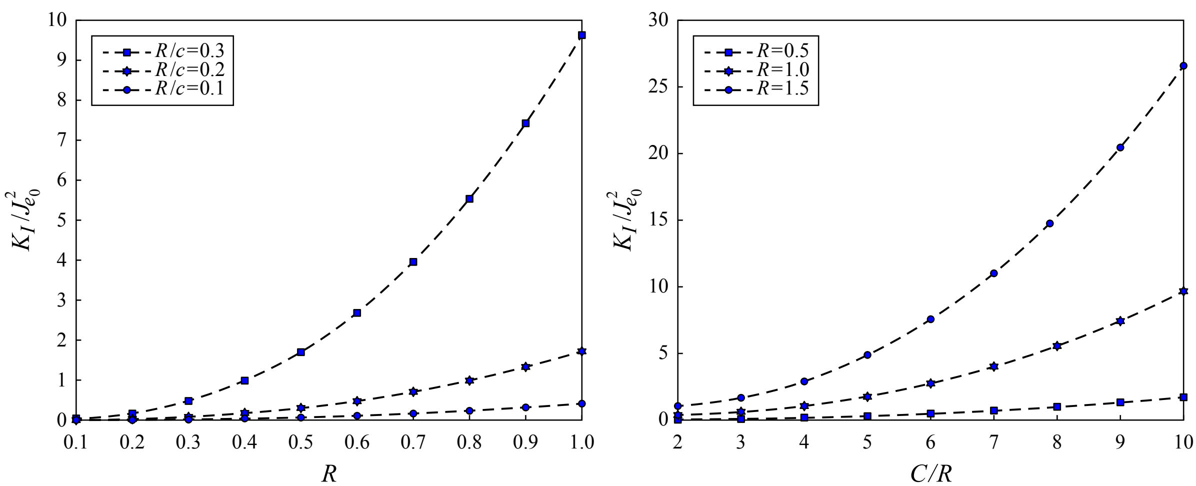

Figure 3. Variation of the stress intensity factor K_I with R (left) and c/R (right).

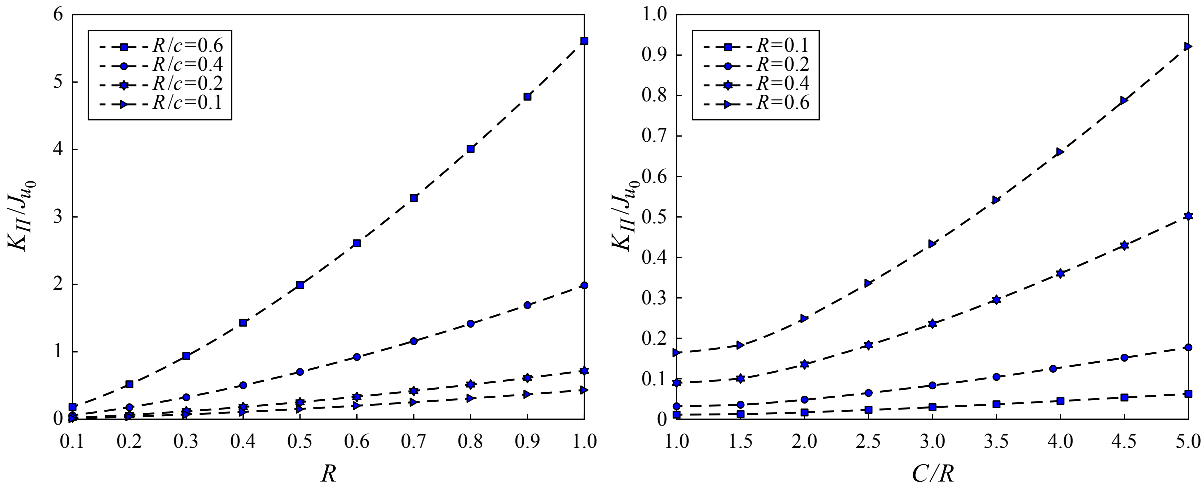

Figure 4. Variation of the stress intensity factor K_{II} with R (left) and c/R (right).

value, the stress intensity factor at the crack tip c increases as the aperture radius increases. When R/c is larger, the rate of K_I increases faster. Figure 4 shows the variation of the stress intensity factor K_{II} with parameters R/c and R. When the radius of the circular hole is larger and the other conditions remain unchanged, the stress intensity factor K_{II} at the crack tip c increases as R increases and the change speed becomes faster with an increase of R/c value. When R is a constant value, the stress intensity factor K_{II} at the crack tip c increases with the increase of c/R, and the change speed becomes faster as c/R increases.

5. Conclusions

Based on the general form of the temperature field and stress field in thermoelectric materials, the explicit solutions of the electric current density and heat flux are obtained by using the complex function method. A more practical case, thermoelectric coupling is considered in this paper. To solve the problem of a circular hole with three cracks, the boundary conditions and conformal mapping were used to map the outer part of the z-plane circular hole to the inner part of the ξ-plane unit circle. The influences of the radius of the hole and the length of the cracks on the electric intensity factor and the stress intensity factor are studied under the condition that the thermoelectric material plate is insulated only by the electric current at infinity.

Acknowledgements

Financial support from the National Natural Science Foundation of China (grants 11762016, 11762017 and 11832014) and the Natural Science Foundation of Ningxia (grant 2020AAC03057) are gratefully acknowledged.

References

[Bertoldi et al. 2007] K. Bertoldi, D. Bigoni, and W. Drugan, "Structural interfaces in linear elasticity, I: Nonlocality and gradient approximations", *J. Mech. Phys. Solids* **55**:1 (2007), 1–34.

[Bigoni and Movchan 2002] D. Bigoni and A. B. Movchan, "Statics and dynamics of structural interfaces in elasticity", *Int. J. Solids Struct.* **39** (2002), 4843–4865.

[Bowie 1956] O. L. Bowie, "Analysis of an infinite plate containing radial cracks originating from the boundary of an internal circular hole", *J. Math. Phys.* (*MIT*) **35** (1956), 60–71.

[Clin et al. 2009] T. Clin, S. Turenne, and D. Vasilevskiy, "Numerical simulation of the thermomechanical behavior of extruded bismuth telluride alloy module", *J. Electro. Mater.* **38**:7 (2009), 994–1001.

[Craciun et al. 2014] E. M. Craciun, T. Sadowski, and A. Răbâea, "Stress concentration in an anisotropic body with three equal collinear cracks in mode II of fracture, I: Analytical study", *Z. Angew. Math. Mech.* **94**:9 (2014), 721–729.

[Ding and Liu 2018] S. H. Ding and Q. N. Liu, "A multi-layered model for heat conduction analysis of thermoelectric material strip", *Comput. Model. Eng. Sci.* **114** (2018), 335–349.

[Ding and Zhou 2018] S. H. Ding and Y. Zhou, "Heat conduction in multilayered thermoelectric materials with multiple cracks", *Acta Mech. Solida Sin.* **4** (2018), 512–522.

[Hone et al. 2013] J. Hone, I. Ellwood, and M. Muno, "Thermoelectric power of single-walled carbon nanotubes", *Phys. Rev. Lett.* **13**:80 (2013), 1335–1338.

[Jiang et al. 2020] D. D. Jiang, Q. H. Luo, W. Liu, and Y. T. Zhou, "Thermoelectric field disturbed by two unequal cracks adjacent to a hole in thermoelectric materials", *Eng. Fract. Mech.* **235** (2020), art. id. 107163.

[Liaw and Kamel 1991] B. M. Liaw and M. Kamel, "A crack approaching a curvilinear hole in an anisotropic plane under general loadings", *Eng. Fract. Mech.* **1** (1991), 25–35.

[Liu et al. 2017] T. Liu, T. Wang, and W. Luan, "Optimal number of thermoelectric couples in a heat pipe assisted thermoelectric generator for waste heat recovery", *J. Electro. Mater.* **46**:5 (2017), 3137–3144.

[Muskhelishvili 1975] N. L. Muskhelishvili, *Some basic problems of mathematical theory of elasticity*, Noordhoff, Leyden, 1975.

[Narasimha et al. 2014] S. Narasimha, P. Taylor, and D. Nemir, "Shockwave consolidation of nanostructured thermoelectric materials", pp. art. id. 92260J in *Nanophotonics and macrophotonics for space environments VIII*, Proc. SPIE **9226**, 2014.

[Ouchterlony 1976] F. Ouchterlony, "Stress intensity factors for the expansion loaded star crack", *Eng. Fract. Mech.* **8** (1976), 447–448.

[Pang et al. 2018] S. J. Pang, Y. T. Zhou, and F. J. Li, "Analytic solutions of thermoelectric materials containing a circular hole with a straight crack", *Int. J. Mech. Sci.* **144** (2018), 731–8.

[Perez-Aparicio et al. 2007] J. L. Perez-Aparicio, R. L. Taylor, and D. Gavela, "Finite element analysis of nonlinear fully coupled thermoelectric materials", *Comput. Mech.* **40**:1 (2007), 35–45.

[Pierce and Vaudo 2010] J. Pierce and R. P. Vaudo, "Methods of depositing epitaxial thermoelectric films having reduced crack and/or surface defect densities and related devices", US patent 7804019 B2, 2010, Available at http://patentscope.wipo.int/search/en/detail.jsf?docId=WO2008097484.

[Roncaglia and Ferri 2011] A. Roncaglia and M. Ferri, "Thermoelectric materials in MEMS and NEMS: a review", *Sci. Adv. Mater.* **3**:3 (2011), 401–419.

[Shi 2020] P. P. Shi, "Singular integral equation method for 2D fracture analysis of orthotropic solids containing doubly periodic strip-like cracks on rectangular lattice arrays under longitudinal shear loading", *Appl. Math. Model.* **77**:2 (2020), 1460–1473.

[Singh et al. 2019] A. Singh, S. Das, and E. M. Craciun, "Effect of thermomechanical loading on an edge crack of finite length in an infinite orthotropic strip", *Mech. Compos. Mater.* **55**:3 (2019), 285–296.

[Song and Song 2016] H. P. Song and K. Song, "Electric and heat conductions across a crack in a thermoelectric material", *J. Theor. Appl. Mech.* (*Warsaw*) **46**:1 (2016), 83–98.

[Song et al. 2015] H. P. Song, C. F. Gao, and J. Y. Li, "Two dimensional problem of a crack in thermoelectric materials", *J. Therm. Stresses* **38**:3 (2015), 325–337.

[Song et al. 2019a] K. Song, H. P. Song, P. Schiavone, et al., "The effects of surface elasticity on the thermal stress around a circular nano-hole in a thermoelectric material", *Math. Mech. Solids* **24** (2019), 3156–3166.

[Song et al. 2019b] K. Song, H. P. Song, P. Schiavone, et al., "The influence of an arbitrarily shaped hole on the effective properties of a thermoelectric material", *Acta Mech.* **230** (2019), 3693–3702.

[Tada et al. 1973] H. Tada, P. C. Paris, and G. R. Irwin, *The stress analysis of cracks handbook*, Del Research, Hellertown, PA, 1973.

[Turenne et al. 2010] S. Turenne, T. H. Clin, and D. Vasilevskiy, "Finite element thermomechanicial modeling of large area thermoelectric generators based on bismuth telluride alloys", *J. Electro. Mater.* **39** (2010), 1926–1933.

[Tweed and Melrose 1989] J. Tweed and G. Melrose, "Cracks at the edge of an elliptic hole in out of plane shear", *Eng. Fract. Mech.* **3** (1989), 743–747.

[Wang 2017] B. L. Wang, "A finite element computational scheme for transient and nonlinear coupling thermoelectric fields and the associated thermal stresses in thermoelectric materials", *Appl. Thermal Engng.* **110** (2017), 136–143.

[Wang and Wang 2017] P. Wang and B. L. Wang, "Thermoelectric fields and associated thermal stresses for an inclined elliptic hole in thermoelectric materials", *Int. J. Eng. Sci.* **119** (2017), 93–108.

[Wang et al. 2014] T. Wang, W. Luan, and W. Wang, "Waste heat recovery through plate heat exchanger based thermoelectric generator system", *App. Energy* **136** (2014), 860–865.

[Wang et al. 2018] P. Wang, K. F. Wang, and B. L. Wang, "Effective thermoelectric conversion properties of thermoelectric composites containing a crack/hole", *Compos. Struct.* **191** (2018), 180–189.

[Wu and Carlsson 1991] X. R. Wu and A. J. Carlsson, *Weight functions and stress intensity factor solutions*, Pergamon, New York, 1991.

[Wu et al. 2018] Y. Wu, H. Zhang, and L. Zuo, "Thermoelectric energy harvesting for the gas turbine sensing and monitoring system", *Energy Conv. Manag.* **157** (2018), 215–223.

[Xie et al. 2017] S. Xie, D. Chen, and M. Gao, "Fracture regularity of thin plate model of main roof with elastic foundation boundary for backfill mining", *J. China Coal Soc.* **42**:9 (2017), 2270–2279.

[Yu et al. 2018] J. Yu, K. Xia, and X. Zhao, "High performance p-type half-Heusler thermoelectric materials", *J. Phys. D Appl. Phys.* **51**:11 (2018), 113001.

[Zhang and Wang 2013] A. B. Zhang and B. L. Wang, "Crack tip field in thermoelectric media", *Theor. Appl. Fract. Mech.* **66**:16 (2013), 33–36.

[Zhang and Wang 2016a] A. B. Zhang and B. L. Wang, "Explicit solutions of an elliptic hole or a crack problem in thermoelectric materials", *Eng. Fract. Mech.* **151** (2016), 11–21.

[Zhang and Wang 2016b] A. B. Zhang and B. L. Wang, "Temperature and electric potential fields of an interface crack in a layered thermoelectric or metal/thermoelectric material", *Int. J. Therm. Sci.* **104** (2016), 396–403.

Received 3 Jul 2020. Revised 10 Aug 2020. Accepted 16 Aug 2020.

QING-NAN LIU: 384831828@qq.com
School of Mathematics and Statistics, Ningxia University, Yinchuan, 750021, China

SHENG-HU DING: dshnx2019@nxu.edu.cn
School of Mathematics and Statistics, Ningxia University, Yinchuan, 750021, China

JOURNAL OF MECHANICS OF MATERIALS AND STRUCTURES

msp.org/jomms

Founded by Charles R. Steele and Marie-Louise Steele

Cover photo: Wikimedia Commons

See msp.org/jomms for submission guidelines.

JoMMS (ISSN 1559-3959) at Mathematical Sciences Publishers, 798 Evans Hall #6840, c/o University of California, Berkeley, CA 94720-3840, is published in 10 issues a year. The subscription price for 2020 is US $660/year for the electronic version, and $830/year (+$60, if shipping outside the US) for print and electronic. Subscriptions, requests for back issues, and changes of address should be sent to MSP.

JoMMS peer-review and production is managed by EditFlow® from Mathematical Sciences Publishers.

PUBLISHED BY

mathematical sciences publishers

nonprofit scientific publishing

http://msp.org/

Journal of Mechanics of Materials and Structures

Volume 15, No. 5 December 2020

1559-3959(2020)15:5;1-H